

Fabrication of $\text{Cu}_3\text{V}_2\text{O}_7(\text{OH})_2 \cdot 2\text{H}_2\text{O}$ Nanoribbons and $\text{Cu}_3\text{V}_2\text{O}_7(\text{OH})_2 \cdot 2\text{H}_2\text{O}/\text{PANI}$ Nanocomposites Used in Supercapacitors

Zhongjie Huang, Wenbin Ni, Huan Pang, Qingyi Lu, Dengchao Wang, and Jianwei Zhao*

Key Laboratory of Analytical Chemistry for Life Science (MOE), School of Chemistry and Chemical Engineering, Nanjing University, Nanjing 210093, P. R. China

(Received October 28, 2009; CL-090957; E-mail: zhaojw@nju.edu.cn)

$\text{Cu}_3\text{V}_2\text{O}_7(\text{OH})_2 \cdot 2\text{H}_2\text{O}$ (CVO) nanoribbons are fabricated through a facile hydrothermal approach, showing a layered structure and multiwater framework proven by TEM, XRD, and FT-IR measurements. The CVO nanoribbon electrode exhibits a specific capacitance of 121 F g^{-1} at a current density of 500 mA g^{-1} in 1.0 M KNO_3 . While PANI materials are both coated on and intercalated into the CVO, the specific capacitance is greatly improved to 197 F g^{-1} .

Supercapacitors are emerging as a novel type of energy-storage device with the potential to substitute for batteries in applications requiring high power densities. Depending on the charge-storage mechanism, supercapacitors can be categorized into two forms: electric double layer capacitors based on carbon materials and pseudocapacitors with certain metal oxides or conducting polymers.¹ Several factors may affect the specific capacitance of the pseudocapacitors. Among them, the material morphology, crystal structure, redox reaction speed, and electrical conductivity are most important. In order to improve the performance of pseudocapacitors, we have designed a novel electrode material, $\text{Cu}_3\text{V}_2\text{O}_7(\text{OH})_2 \cdot 2\text{H}_2\text{O}$ (CVO). Through controlling the synthesis conditions, we hope to modulate the material morphology and crystal structure in the nanometer scale. Then we will gain the correlation of these properties with the material performance used in supercapacitors. For further improving the electrical conductivity between the electroactive CVO and the inert electrode, we have introduced the polyaniline (PANI).

CVO nanoribbons have many unique features: low-dimensional morphology, layered structure, a multiwater framework and various chemical valences for reversible redox reaction. The faster charge transport in the 1-D nanostructure is essential for achieving higher charging/discharging rate.² It also possesses a structure made up of $\text{Cu}-\text{O}(\text{OH})$ layers pillared by pyrovanadate groups V_2O_7 with water molecules embedded between the layers.^{3,4} This structure allows the efficient and reversible intercalation of a variety of ions.⁵ In addition, the various chemical valences (II, III, IV, and V) of vanadium provide several oxidation states, paramount for pseudocapacitors deriving from the reversible redox transitions of the electroactive materials. Therefore, CVO might have promising application in supercapacitors, though this material has rarely been reported for the application in pseudocapacitors.

CVO nanoribbons were synthesized through a facile hydrothermal route from the reaction of 92.1 mg of $\text{CuCl}_2 \cdot 2\text{H}_2\text{O}$ and 42.1 mg of NH_4VO_3 in a 30-mL Teflon-lined autoclave at 200°C for 12 h. CVO/PANI nanocomposites were obtained by an in situ method using CVO as a reactive template and oxidant for aniline polymerization in an ice bath. Morphology character-

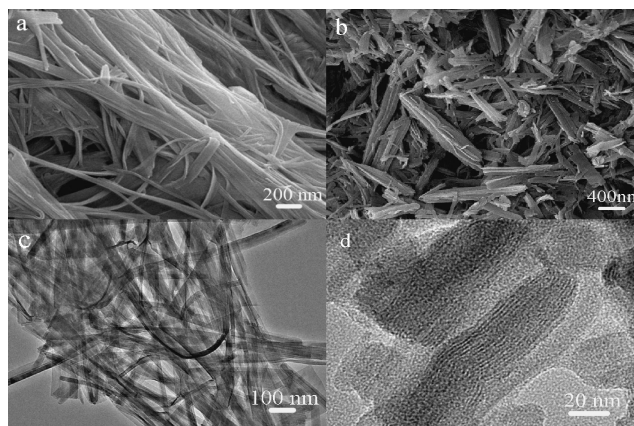


Figure 1. SEM images of CVO nanoribbons (a) and CVO/PANI nanocomposites (b), TEM images of CVO nanoribbons (c) and CVO/PANI nanocomposites (d).

ization was performed with a scanning electron microscope (SEM, S-4800, Hitachi) and a high-resolution transmission electron microscope (HRTEM, JEM-2100, Jeol). Fourier transform infrared spectroscopy (FTIR, NicLET 6700, Thermo scientific) and powder X-ray diffraction (XRD, XRD-6000 diffractometer, Shimadzu) were used for structural investigation. The electrochemical measurements were carried out using a three-electrode electrochemical cell with the help of a CHI660B (Shanghai Chenhua Apparatus, China) electrochemical workstation.

The morphology characters of the synthesized CVO nanoribbons and CVO/PANI nanocomposites are presented by SEM and TEM images in Figure 1. Figure 1a shows the ribbon-like morphology of CVO. Figure 1c reveals that the CVO nanoribbons have uniform widths in the range of 30–70 nm along their entire length, which can be up to a few micrometers. This uniformity might be important for the potential application in electronic devices. After reaction with the aniline, most of the nanoribbons are somewhat fractured and coated by PANI layers, as demonstrated by Figure 1b. Figure 1d gives a clearer view of the layered structure of CVO and the coated PANI layers. The interplanar distance of the nanocomposite is expanded to 2.14 nm, much larger than that of pure CVO,³ revealing that PANI is not only coated on the outer surface but also intercalated into the layered structure of CVO matrix.

XRD was used to identify the crystalline phase of the prepared samples. The narrow and strong diffraction peaks of CVO in Figure 2a can be indexed to the pure phase of CVO with monoclinic layered structure [JCPDS-ICDD Card No. 80-1170]. The CVO/PANI nanocomposites have no such clear sharp peaks, implying their amorphous nature. The structural infor-

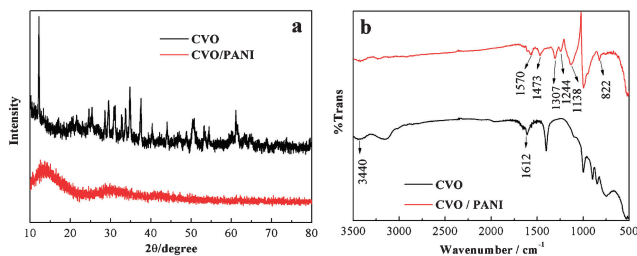


Figure 2. XRD patterns (a) and FTIR spectra (b) of CVO nanoribbons and CVO/PANI nanocomposites.

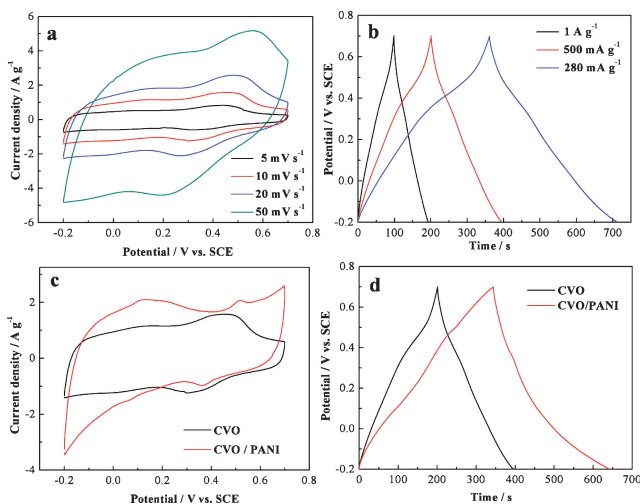


Figure 3. CV (a) and charge-discharge curves (b) of CVO nanoribbons in a potential range from -0.20 to 0.70 V (vs. SCE), CV curves of CVO nanoribbons and CVO/PANI nanocomposites under a scan rate of 10 mV s^{-1} (c), charge-discharge curves of CVO nanoribbons and CVO/PANI nanocomposites at a current density of 500 mA g^{-1} (d).

mation of samples was further identified by the FTIR spectra (Figure 2b). The FTIR spectrum of CVO is similar to that reported previously.⁶ The peaks at 3440 and 1612 cm^{-1} are ascribed to the stretching and bending vibrations of H_2O molecules, illustrating the multiwater framework of CVO. As to the nanocomposites, the stretching vibration peaks of quinoid ring and benzenoid ring at 1570 and 1473 cm^{-1} , the C–N stretching bands at 1307 and 1244 cm^{-1} , and other characteristic peaks at 1138 and 822 cm^{-1} all indicate the presence of PANI.^{7,8}

Electrochemical properties were investigated by cyclic voltammetry (CV) and chronopotentiometry (CP) tests. Figure 3a shows the CV curves of CVO electrode under different scan rates in a potential range from -0.20 to 0.70 V (vs. SCE) in 1.0 M KNO_3 electrolyte. The potential window of CVO is relatively wide, which is promising for application in supercapacitors in aqueous solution. A rapid rise/decay in current is clearly found while the potential scan direction changes, revealing that the charge/discharge processes together with faradic reactions occurring in the electrode are relatively fast and reversible. The peaks in the curves indicate the insertion and extraction of active K^+ ions in the redox process.⁹ Figure 3b depicts the charge/discharge curves for CVO nanoribbons

between -0.2 and 0.7 V (vs. SCE) at different current densities. The specific capacitance (SC) values of CVO nanoribbons are 124 , 121 , and 120 F g^{-1} for different current densities of 0.28 , 0.5 , and 1.0 A g^{-1} , respectively. This value is not as prominent as RuO_2 but comparable to other metal oxide such as NiO and Fe_3O_4 .^{10,11}

To improve the performance and get deeper insight into the supercapacitor materials, we have made further improvements by preparing CVO/PANI nanocomposite. Figure 3c compares the CV curves of CVO and nanocomposites at a scan rate of 10 mV s^{-1} . The CV curve of the nanocomposites is more rectangular, as expected for the ideal capacitor behavior. Especially in the potential range over 0.5 V, the nanocomposites display a better electrochemical performance. Moreover, the nanocomposites have much larger current density than CVO, indicating higher SC values. Figure 3d shows the charge-discharge curves of CVO and nanocomposites at a current density of 500 mA g^{-1} . The SC value of CVO/PANI nanocomposites is improved up to 197 F g^{-1} , much higher than that of CVO nanoribbons, 121 F g^{-1} .

The fabrication of hybrid CVO/PANI electrode leads to large enhancement of SC. This can be attributed to several reasons. First, PANI improves the electrical conductivity and electrochemical stability of the electrode material. Second, the swollen layered structure resulting from PANI intercalation can improve the diffusion rate of electrolyte ions.¹² Finally, the existence of coated PANI layers helps to maintain the layered structure and nanoarchitecture of CVO during charge-discharge, which is beneficial to obtaining high SC values.

In conclusion, we have synthesized a kind of CVO nanoribbon material and its nanocomposites with conducting polymer using a facile hydrothermal approach. Electrochemical tests show that CVO-based nanocomposites are promising for supercapacitor materials.

References

- 1 B. E. Conway, *Electrochemical Supercapacitors: Scientific Fundamentals and Technological Applications*, Kluwer Academic/Plenum, New York, **1999**.
- 2 S. Passerini, J. J. Ressler, D. B. Le, B. B. Owens, W. H. Smyrl, *Electrochim. Acta* **1999**, *44*, 2209.
- 3 Z. Hiroi, M. Hanawa, N. Kobayashi, M. Nohara, H. Takagi, Y. Kato, M. Takigawa, *J. Phys. Soc. Jpn.* **2001**, *70*, 3377.
- 4 S. Y. Zhang, L. J. Ci, H. R. Liu, *J. Phys. Chem. C* **2009**, *113*, 8624.
- 5 C. R. Xiong, A. E. Aliev, B. Gnade, K. J. Balkus, *ACS Nano* **2008**, *2*, 293.
- 6 K. Melghit, A. H. Yahaya, I. I. Yaacob, *Mater. Lett.* **2003**, *57*, 1423.
- 7 Z. M. Zhang, Z. X. Wei, M. X. Wan, *Macromolecules* **2002**, *35*, 5937.
- 8 H. Ding, M. Wan, Y. Wei, *Adv. Mater.* **2007**, *19*, 465.
- 9 R. N. Reddy, R. G. Reddy, *J. Power Sources* **2006**, *156*, 700.
- 10 Y.-Z. Zheng, H.-Y. Ding, M.-L. Zhang, *Mater. Res. Bull.* **2009**, *44*, 403.
- 11 J. Chen, K. L. Huang, S. Q. Liu, *Electrochim. Acta* **2009**, *55*, 1.
- 12 Y.-G. Wang, W. Wu, L. Cheng, P. He, C.-X. Wang, Y.-Y. Xia, *Adv. Mater.* **2008**, *20*, 2166.